# Extended common-image-point gathers for anisotropic wave-equation migration

Paul Sava (Colorado School of Mines) and Tariq Alkhalifah (KAUST)

## Introduction

In regions characterized by complex subsurface structure, wave-equation depth migration is a powerful tool for accurately imaging the earth's interior. The quality of the final image greatly depends on the quality of the model which includes anisotropy parameters (Gray et al., 2001). In particular, it is important to construct subsurface velocity models using techniques that are consistent with the methods used for imaging. Generally speaking, there are two possible strategies for velocity estimation from surface seismic data in the context of wavefield-based imaging (Sava et al., 2010). One possibility is to formulate an objective function in the *data space*, prior to migration, by matching the recorded data with simulated data. Techniques in this category are known by the name of waveform inversion. Another possibility is to formulate an objective function in the *image space*, after migration, by measuring and correcting image features that indicate model inaccuracies. Techniques in this category are known as wave-equation migration velocity analysis (MVA).

The key component for an MVA technique implemented in the image space is the analysis of image attributes which indicate inaccurate imaging. These attributes are often represented by image extensions, e.g. reflectivity as functions of angle or offset which exploit the semblance principle stating that images constructed for different seismic experiments are kinematically similar if the correct velocity is used. This property can be exploited for velocity model building by minimizing objective functions to optimize certain image attributes. For example, we can consider flatness or focusing measured on image gathers Symes (2009). The analysis of image attributes is more critical in anisotropic media, as the model is described by more than one parameter.

In transversely isotropic (TI) with vertical symmetry axis (VTI) media, the acoustic problem can be described by three parameters (Alkhalifah and Tsvankin, 1995): the vertical velocity, the NMO velocity, and the anisotropy parameter $\eta$ that relates the NMO velocity to the horizontal velocity. In this case, however, the recorded data contain information on only the NMO velocity and $\eta$ (Alkhalifah and Tsvankin, 1995), and thus, the vertical velocity is not resolved. This fact holds for complex anisotropy, but at a lesser extent (Alkhalifah et al., 2001). However, since the stratification in the Earth subsurface is not always horizontal, we can expect the symmetry axis to have some deviation from the vertical especially around, for example, salt-body flanks. For TI media with a tilt in the axis of symmetry two additional parameters, $\theta$ and $\alpha$ that describe the tilt in 3-D, are needed to fully characterize acoustic wave propagation. These two parameters are often estimated by assuming that the tilt direction is normal to the medium structure or in the direction of the velocity gradient (Alkhalifah and Bednar, 2000; Audebert et al., 2006). Alkhalifah and Sava (2010) use this fact to develop equations to describe imaging in media in the which the tilt of the symmetry axis is normal to the reflector dip.

An image obtained by wave-equation migration can be extracted from the reconstructed wavefields by the application of an extended imaging condition:

$$R\left(\mathbf{x},\boldsymbol{\lambda},\tau\right)=\sum_{shots}\sum_{\omega}\overline{W_s\left(\mathbf{x}-\boldsymbol{\lambda},\omega\right)}W_r\left(\mathbf{x}+\boldsymbol{\lambda},\omega\right)e^{2i\omega\tau}\ . \tag{1}$$

The image $R$ is a function of the space coordinates $\mathbf{x}$, and of the space- and time-lag extensions, $\boldsymbol{\lambda}$ and $\tau$ (Rickett and Sava, 2002; Sava and Fomel, 2006). For correct velocity, events corresponding to all experiments focus at zero space- and time-lags (Sava and Vasconcelos, 2009). In this abstract, we

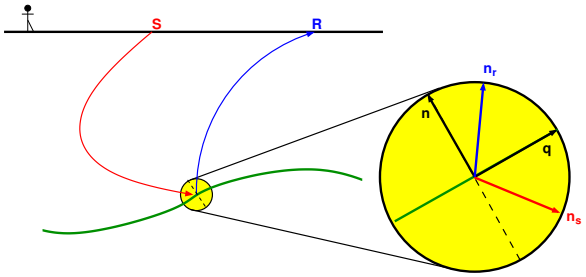


Figure 1: Cartoon illustrating the assumptions made in deriving the moveout functions based on space-lag and time-lag extensions.

analyze the properties of such extended images constructed using TI anisotropic models and we explore their usability for wave-equation anisotropic model building.

**Moveout analysis**

Consider the reflection geometry depicted in Figure 1. In the immediate vicinity of the reflection points, we can assume that the source wavefield, the receiver wavefield and the reflector itself can be approximated by planes and we can also assume that the local velocity in this region is constant. This is especially convenient for anisotropic media as plane waves in this case are dependent on the phase velocity, which can be described explicitly (Alkhalifah, 1998). The source, receiver and reflector planes are characterized by unit vectors $\mathbf{n}_s$, $\mathbf{n}_r$, and $\mathbf{n}$, respectively. The vectors are linked according to Snell's law by the relations:

$$|\mathbf{n}_s \cdot \mathbf{n}| = |\mathbf{n}_r \cdot \mathbf{n}|; , \tag{2}$$

where $\theta$ represents the reflection angle measured relative to the reflector normal $\mathbf{n}$.

For a specific reflection event, without loss of generality, we can set the origin of the time axis at the moment when the two planes characterizing the source and receiver wavefields planes intersect at the reflector. Then, we can write the expressions for the source and receiver wavefield planes as

$$\mathbf{n}_s \cdot \mathbf{x} = 0 , \tag{3}$$
$$\mathbf{n}_r \cdot \mathbf{x} = 0 , \tag{4}$$

where $\mathbf{x}$ is a variable spanning the planes. By construction, the extended imaging condition separates the source and receiver wavefield by shifts in space and time using quantities $\boldsymbol{\lambda}$ and $\tau$, respectively. The expressions for the shifted planes for a general anisotropic medium in space and time are

$$\mathbf{n}_s \cdot (\mathbf{x} - \boldsymbol{\lambda}) = -v(\theta_s)\tau , \tag{5}$$
$$\mathbf{n}_r \cdot (\mathbf{x} + \boldsymbol{\lambda}) = +v(\theta_r)\tau , \tag{6}$$

where $v$ represents the local phase velocity at the reflection point for the incidence $\theta_s$ and reflection $\theta_r$ phase angles, assumed to be constant in the region in which the planar assumptions on the source and receiver wavefields holds. If we constrain the tilt of the TI symmetry axis to be normal to the dip, applying what Alkhalifah and Sava (2010) referred to as the DTI constraint, then the incidence and reflection angles are always equal, $\theta = \theta_s = \theta_r$, where $\theta$ is the reflection angle. In this case, subtracting the expressions 5-6, we obtain

$$(\mathbf{n}_r + \mathbf{n}_s) \cdot \boldsymbol{\lambda} = 2v(\theta)\tau . \tag{7}$$

If we define unit vector $\mathbf{q}$ in the reflection plane, tangent to the reflector, then we can write

$$(\mathbf{q} \cdot \boldsymbol{\lambda}) \sin\theta = v(\theta)\tau . \tag{8}$$

Equation 8 describes the moveout function characterizing a reflection from a shot-receiver pair in the $\{\boldsymbol{\lambda}, \tau\}$ space, i.e. the space- and time-lags are linearly related by a function which depends on $\theta$, the local velocity $v$, and by vector $\mathbf{q}$ which depends on the reflector dip and reflection azimuth (Figure 3(a)).

We can express the moveout function $s(\boldsymbol{\lambda}, \tau)$ for a single shot-receiver pair using the multidimensional Dirac delta function as (Bracewell, 2006):

$$s(\boldsymbol{\lambda}, \tau) = \delta\left((\mathbf{q} \cdot \boldsymbol{\lambda}) \sin\theta - v(\theta)\tau\right) . \tag{9}$$

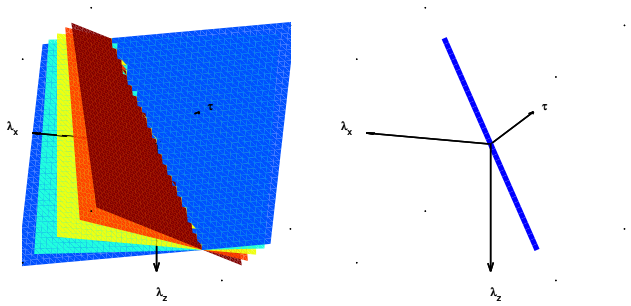


(a) (b)

Figure 2: Illustration of (a) the reflection moveout function for individual shots, (b) the reflection moveout function for all shots. Panels (a) and (b) correspond to a reflector dipping at 15°. Panel (a) assumes angles of incidence from −60° to +60°.

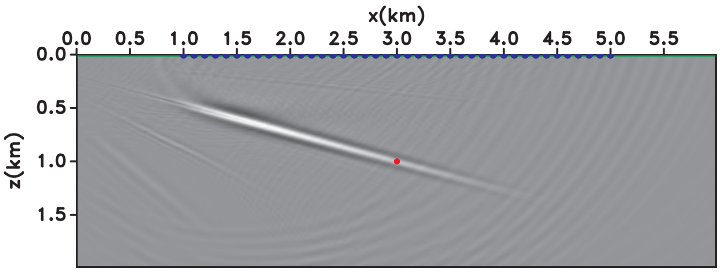


Figure 3: The image constructed in a VTI model using correct anisotropy parameters.

This expression simply indicates that $s(\boldsymbol{\lambda}, \tau) = 1$ when $(\mathbf{q} \cdot \boldsymbol{\lambda}) \sin\theta = v(\theta)\tau$ and $s(\boldsymbol{\lambda}, \tau) = 0$ otherwise. The moveout characterizing in the $\{\boldsymbol{\lambda}, \tau\}$ space a reflection from many shots located on the surface is given by the superposition of events from different sources, i.e. we construct the moveout function $r(\boldsymbol{\lambda}, \tau)$ by integration over all possible values of the angle $\theta$, therefore

$$r(\boldsymbol{\lambda}, \tau) = \delta(\mathbf{q} \cdot \boldsymbol{\lambda})\, \delta(v(\theta)\tau) \ . \tag{10}$$

Equation 10 indicates that the moveout function characterizing a reflector illuminated from many shots is a line at $\tau = 0$ oriented at an angle parallel to the reflector normal (Figure 3(b)). Such events can be seen in Figure 4(d) for the case of the horizontal reflector shown in Figure 3.

### Synthetic example

We illustrate the behavior of the CIPs described in the preceding section using a simple model of a horizontal reflector embedded in a VTI model characterized by parameters $v_v = v_{NMO} = 3.0$ km/s and $\eta = 0.3$. Figure 3 shows a conventional image obtained by anisotropic migration with correct $\eta$. Figures 4(d)-4(h) show extended images obtained by imaging with correct and incorrect $\eta$, respectively, at the location indicated by the dot on the conventional images. The extended images are represented by a single event oriented in the $\boldsymbol{\lambda}$ panel at an angle orthogonal to the reflector. Likewise, Figures 4(a)-4(g) show the CIPs constructed at the same location for individual shots. In all cases, the moveout function for an individual shot is a plane in the $\{\boldsymbol{\lambda}, \tau\}$ space depending on the angle of incidence and local velocity. Furthermore, if the anisotropy parameters are incorrect, then the CIPs show events characterized by moveout which can be used for model updates using a tomographic procedure.

### Conclusions

Extended common-image-point gathers are effective tools for analyzing model accuracy for wave-equation imaging. The extended CIPs can be analyzed at sparse locations in the image volume, thus reducing the computational cost of this imaging condition. A key requirement for the effectiveness of this technique is that space-lags and time-lag extensions be analyzed simultaneously. For dip-constrained TI media, the CIP moveout formula is similar to the one developed in isotropic media but uses the phase angle instead of the reflection angle. Furthermore, the extended CIPs are sensitive to errors in the anisotropy parameters and can form the basis for wavefield-based tomographic model updates.

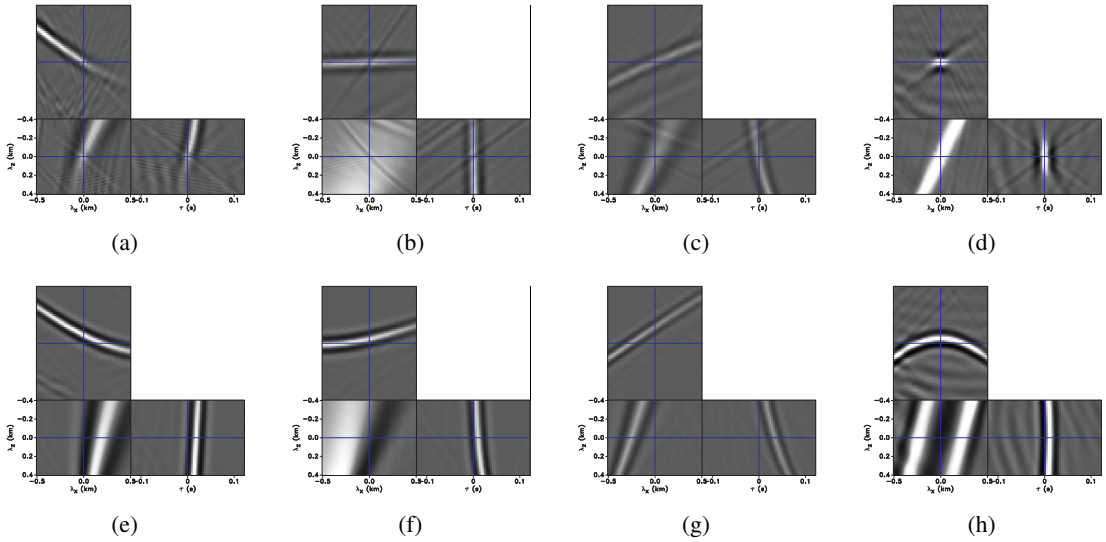

Figure 4: CIPs constructed at subsurface coordinates $z = 1$ km and $x = 3$ km. Panels (a)-(d) and (e)-(h) correspond to imaging with correct and incorrect anisotropy parameters, respectively. Panels (d) and (h) are stacks for all shots on the surface, and the other panels correspond to individual shots.

**Acknowledgments**

P. Sava acknowledges the support of the sponsors of the Center for Wave Phenomena at Colorado School of Mines. T. Alkhalifah thanks KAUST for their support.

**REFERENCES**

Alkhalifah, T., 1998, Acoustic approximations for processing in transversely isotropic media: Geophysics, **63**, 623–631.

Alkhalifah, T., and J. Bednar, 2000, Building a 3-D anisotropic model: Its implications to traveltime calculation and velocity analysis: 70th Ann. Internat. Mtg, Soc. of Expl. Geophys., 965–968.

Alkhalifah, T., S. Fomel, and B. Biondi, 2001, The space-time domain:theory and modelling for anisotropic media: Geophysical Journal International, **144**, 105–113.

Alkhalifah, T., and P. Sava, 2010, A transversely isotropic medium with a tilted symmetry axis normal to the reflector: Geophysics, submitted.

Alkhalifah, T., and I. Tsvankin, 1995, Velocity analysis for transversely isotropic media: Geophysics, **60**, 1550–1566.

Audebert, F., D. V., and P. A., 2006, Tti anisotropic depth migration: What tilt estimate should we use?: SEG, Expanded Abstracts, **25**, 2382–2386.

Bracewell, R., 2006, Fourier analysis and imaging: Springer.

Gray, S. H., J. Etgen, J. Dellinger, and D. Whitmore, 2001, Seismic migration problems and solutions: Geophysics, **66**, 1622–1640.

Rickett, J., and P. Sava, 2002, Offset and angle-domain common image-point gathers for shot-profile migration: Geophysics, **67**, 883–889.

Sava, P., and S. Fomel, 2006, Time-shift imaging condition in seismic migration: Geophysics, **71**, S209–S217.

Sava, P., P. Fowler, and U. Albertin, 2010, Objective functions for seismic wavefield tomography: Geophysics (Letters), submitted for publication.

Sava, P., and I. Vasconcelos, 2009, Extended imaging condition for wave-equation migration: Geophysical Prospecting, submitted for publication.

Symes, W., 2009, Migration velocity analysis and waveform inversion: Geophysical Prospecting, **56**, 765–790.